SURFACE ROUGHNESS PREVENTS SHARAD PENETRATION OF SOME MARTIAN DEBRIS-COVERED GLACIERS: A FRACTAL ANALYSIS OF HIRISE DTMS E. I. Petersen[1] and J. W. Holt[1] [1]Lunar and Planetary Laboratory, University of Arizona, Tucson AZ (petersen@lpl.arizona.edu)

Introduction: Debris-covered glaciers (DCG) are numerous in the mid-latitudes of Mars and are targets of high interest for in-situ resource utilization of water ice, as well as a record of Amazonian climate [1-5].

The Shallow Radar (SHARAD) sounding instrument onboard Mars Reconnaissance Orbiter (MRO) detects the base of many DCG and has been used in previous studies [3,4] to constrain their bulk composition (>80% water ice with surface debris 1-10 m thick). A recent expanded survey in the region of Deuteronilus Mensae showed that these results are consistent for 87% of DCG surveyed, while the remaining 13% lacked detection of the base or interior of DCG (Figures 1-2) [6].

One possible explanation is the rough sublimation pit textures that are typically found on DCG surfaces [7]. DCG with exceptionally rough surfaces may scatter the incident radar signal such that any reflection from basal or interior interfaces is reduced to below SHARAD's noise level.

In this study we quantify DCG surface roughness using a fractal model applied to high resolution digital terrain models (DTMs).

Methods: The High Resolution Imaging Science Experiment (HiRISE) is a visible and near infrared imager on board MRO capable of resolutions up to 25 cm. The resolution of HiRISE allows us to accurately quantify topography on the scales relevant to SHARAD. We produced digital terrain models (DTMs) at 1 m resolution from stereo HiRISE imaging at five DCG sites using the open source NASA Ames Stereo Pipeline [8,9].

For each DTM that was produced, patches where extracted that correspond to the effective footprint of individual SHARAD observations (Figures 3, 4a). These patches thus represent the surface roughness relevant to each observation, whether it produced a detection or non-detection of subsurface signal.

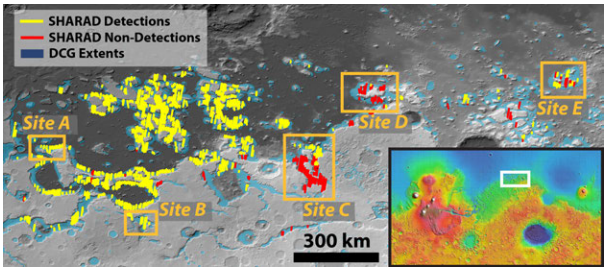

Figure 1: *Map of Deuteronilus Mensae DCGs with basal detections and non-detections mapped in SHARAD, indicating where the subsurface is visible and invisible respectively. Study sites A-E with available stereo HiRISE DTMs are shown. (Inset) Mars MOLA map with location of study site.*

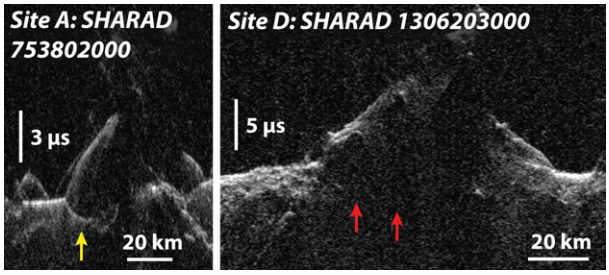

Figure 2: *Sample radargrams from Site A and Site D showing examples of detection (yellow arrow) and non-detection (red arrows) of radar echoes from the base of the DCG.*

We then employed a fractal model developed by [10] to quantify DCG surface roughness for each of these footprints using the rms surface slope parameter $s(\Delta x)$:

$$s(\Delta x) = \frac{\sqrt{\langle (z(x) - z(x+\Delta x))^2 \rangle}}{\Delta x} \quad (1)$$

Where z is detrended surface slope and x the horizontal location along any profile. The rms surface slope is dependent upon horizontal scale Δx and follows an exponential form dependent upon an anchoring rms slope at the scale of the radar wavelength s_λ as well as the hurst exponent H:

$$s(\Delta x) = s_\lambda (\frac{\Delta x}{\lambda})^{H-1} \quad (2)$$

s_λ is arguably the most important parameter, while H (values between 0 and 1) describes how roughness increases at greater lengths scales. A least-squares fit of the form shown in Eqn. 2 was then applied to solve for H (Figure 4).

The radar backscattering coefficient is derived:

$$\sigma_0(H) = 16\pi^3 \rho [\int_{\hat{r}=0}^{\infty} exp[-4\pi^2 s_\lambda \hat{r}^{2H} cos^2\theta] \hat{r} \times J_0(4\pi \hat{r} sin(\theta)) d\hat{r}]^2 \quad (3)$$

Where ρ is the assumed surface reflectivity and θ the incidence angle.

Results: The rms slope $s(\Delta x)$ for each SHARAD footprint was fit well by equation 2, with all fits featuring $R^2 > 0.91$. H ranges between 0.24 and 0.62, while s_λ ranges between 2.6° and 5.6°–corresponding to rms height of 0.4-1.0 m. The difference in roughness between DCG surfaces is a result of glacial and periglacial

textures including sublimation pits (strong effect on s_λ) and flow lineations/troughs (strong effect on H).

SHARAD observations that were mapped as non-detections generally exhibit values of $s_\lambda > 3.75°$, while detections tend to have values lower than $3.75°$ (Figure 5). Non-detections with lower values of s_λ tend to exhibit higher H values. The dividing line in H-s_λ parameter space between detections and non-detections roughly follows the contour of σ_0 = 60 dB.

Discussion and Conclusions: There is a strong correlation between surface roughness and the detectability of the subsurface in SHARAD data over DCG. Surfaces with a theoretical backscatter $\sigma_0 > 60$ dB are nearly all non-detections while surfaces with $\sigma_0 < 60$ dB are nearly all detections. This work thus shows that surface roughness alone is sufficient to explain the differences in SHARAD detectability of DCG interiors.

The morphologies controlling DCG surface roughness have been linked to glacial and periglacial processes [11]. This line of evidence, and the similar gross morphology between DCG with and without SHARAD detections, leads us to interpret these features as equivalent in terms of internal composition (>80% water ice).

References: [1] Head, J., et al. (2009), EPSL, 294, 306-320. [2] Squyres, S. (1979), JGR: Solid Earth, 84, 8087-8096 [3] Holt, J., et al. (2008), Science, 322, 1235-1238. [4] Plaut, J., et al. (2009), GRL 36. [5] Levy, J., et al. (2014), JGR: Planets, 119(10), 2188-2196, [6] Petersen et al. (2018), GRL 45(21), 11,595-11,604, [7] Mangold (2003), JGR: Planets 108(E4), [8] Broxton and Edwards (2008), LPSC 39, 2419, [9] Moratto et al. (2010), LPSC 41, 2364, [10] Shepard and Campbell (1999), Icarus 141(1), 156-171, [11] Levy, J., et al. (2009), Icarus 202(2), 462-476.

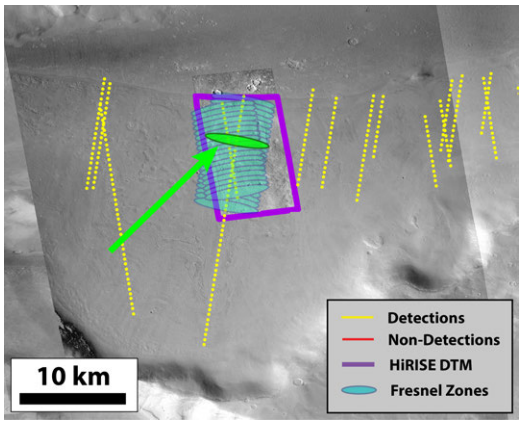

Figure 3: *Context map for Site A (Location in Fig. 1) showing the location of the stereo HiRISE DTM and overlapping SHARAD Fresnel zones corresponding to detections of the glacier interior. Example Fresnel zone shown in Figure 4 is highlighted in green.*

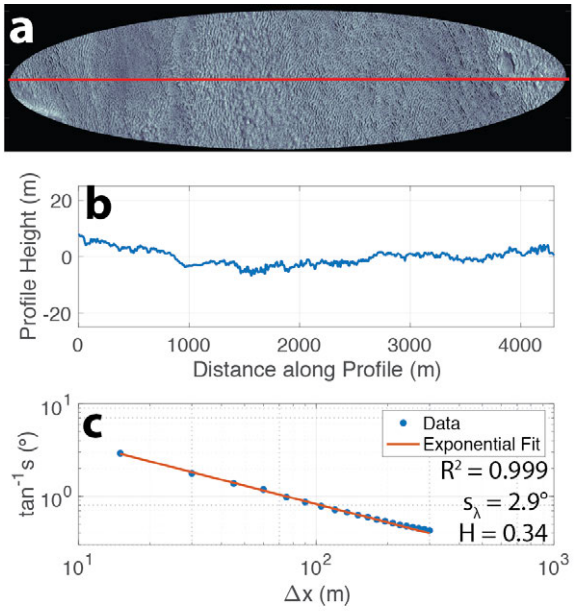

Figure 4: *Example profile analysis of topography within a Fresnel zone sample of the stereo HiRISE DTM. (a) HiRISE image of Fresnel zone; red line indicates the location of the (b) detrended elevation profile. (c) RMS surface slope $tan^{-1}s_\lambda$ as a function of Δx; fractal concepts have been applied to solve for the hurst exponent H.*

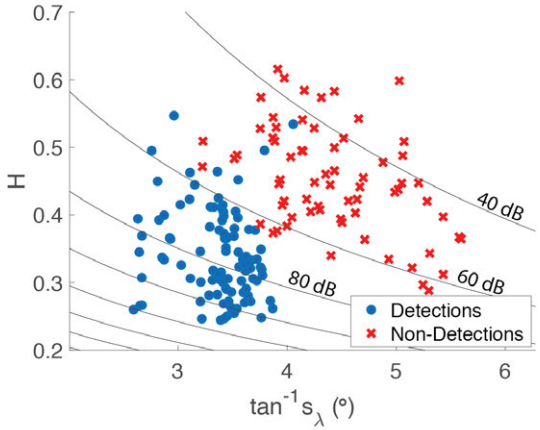

Figure 5: *Hurst exponent H plotted against the rms surface slope $tan^{-1}s_\lambda$ to present the results of fractal surface roughness analysis for all SHARAD Fresnel zones overlapping HiRISE DTMs in Sites A-E. Detections of the glacier basal interface tend to correspond with surfaces less rough in $tan^{-1}s_\lambda$, H, or both while non-detections correspond to rougher surfaces. Contours indicate the theoretical backscattering coefficient σ_0 for surfaces with these values of $tan^{-1}s_\lambda$ and H (Eqn. 3).*